The Hydride Anion in an Extended Transition Metal Oxide Array: $LaSrCoO_3H_{0.7}$

M. A. Hayward,[1] E. J. Cussen,[1] J. B. Claridge,[1] M. Bieringer,[1] M. J. Rosseinsky,[1]* C. J. Kiely,[1,2] S. J. Blundell,[3] I. M. Marshall,[3] F. L. Pratt[4]

We present the synthesis and structural characterization of a transition metal oxide hydride, $LaSrCoO_3H_{0.7}$, which adopts an unprecedented structure in which oxide chains are bridged by hydride anions to form a two-dimensional extended network. The metal centers are strongly coupled by their bonding with both oxide and hydride ligands to produce magnetic ordering at temperatures up to at least 350 kelvin. The synthetic route is sufficiently general to allow the prediction of a new class of transition metal–containing electronic and magnetic materials.

The covalent interaction between the O^{2-} anion and the d orbitals of the transition metal cation is at the heart of the remarkable electronic properties of the transition metal oxides (*1*, *2*). Even in mixed-anion oxyhalides (*3*), it is the metal-oxide interactions that dominate the physical properties. Developing synthetic routes to materials in which other anions partially replace oxide could open up the possibility of preparing entirely novel families of electronically active transition metal compounds. The hydride anion, H^-, with a $1s^2$ electronic configuration, is known to engage in strong covalent bonding with transition metal centers in discrete molecular species (*4*) and would be an excellent candidate for the transmission of exchange interactions or electron delocalization among transition metal cations in an oxide hydride, if the formidable synthetic difficulties barring the path to such a phase could be overcome. The problem is that H^-, unlike O^{2-} or halide anions such as F^- and Cl^-, is a powerful reducing agent and would be expected to transform the transition metal component of a typical high-temperature ternary transition metal oxide synthesis into the metal, defeating most possible synthetic strategies. Here, we demonstrate a low-temperature topotactic route to the insertion of H^- anions directly into an extended transition metal oxide array and show that H^- transmits exchange interactions among the transition metal cations at least as effectively as O^{2-}, opening up a new mechanism for designing cooperative effects in solids.

We have recently shown that NaH is an effective low-temperature reducing agent for ternary transition metal oxides. At temperatures below 190°C, NaH affords the Ni(I) (*5*) and Co(I) (*6*) oxidation states, but at higher temperatures completely reduces the metal because of the presence of hydrogen gas in thermal equilibrium with the hydride salt. To study the solid-state reactivity of H^- with ternary transition metal oxides at higher temperatures, we used the more thermally stable CaH_2 (with a decomposition temperature of 885°C, as compared with 210°C for NaH). CaH_2 was reacted with the Co(III) oxide $LaSrCoO_4$, which adopts the layered K_2NiF_4 structure with square planar CoO_2 sheets alternating with (La/Sr)O rock salt layers and octahedral coordination around Co(III). Reaction for two periods of 4 days at 450°C in a sealed Pyrex tube with intermediate grinding afforded a mixture of CaO and an orthorhombic phase **1** (*7*). The orthorhombic phase is structurally related to the starting material, and its lattice parameters suggest a one-dimensional (1D) Sr_2CuO_3 structure that consists of chains of corner-sharing MO_4 squares (*7*). The transformation to such a structure suggests that **1** is the Co(I) phase $LaSrCoO_3$, formed by the reductive topotactic extraction of O^{2-} to afford CaO. CaO was removed from **1** by washing with 0.1 M NH_4Cl in degassed methanol under nitrogen and then filtering and drying under vacuum. The structure and composition of **1** were investigated by powder synchrotron x-ray diffraction (XRD), neutron diffraction, and selected-area electron diffraction (SAED).

The 290 K synchrotron XRD pattern was readily indexed with the orthorhombic Sr_2CuO_3-type unit cell in the *Immm* space group, an assignment confirmed by SAED (*7*). Structural refinement showed that the cations occupy the metal positions expected for the Sr_2CuO_3 structure. The ambient temperature neutron powder diffraction data, however, could not be indexed on this basis; a doubling of the basal *ab* plane area was required to account for additional diffraction reflections observed at large d-spacings. The absence of these reflections in the XRD and SAED data, which would be sensitive to superstructure formation

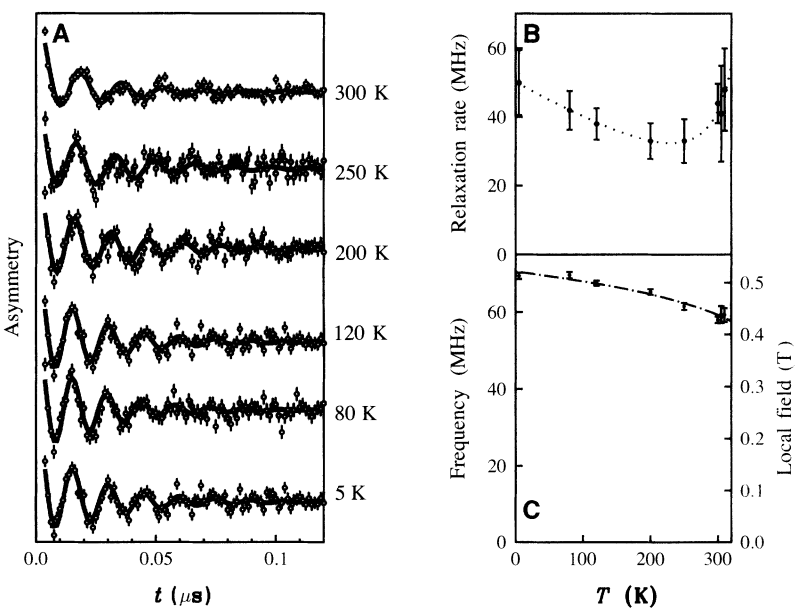

Fig. 1. (**A**) μSR data from **1**. The oscillations in the asymmetry demonstrate long-range magnetic order at all temperatures measured (up to 310 K). (**B**) Temperature dependence of the relaxation rate of the oscillations (the dotted line is a guide to the eye). (**C**) Temperature dependence of the μSR frequency and the corresponding magnetic field at the muon site. In (C), the line represents a fit to a phenomenological expression for the temperature dependence of the order parameter in a magnetic material. Good fits could be obtained by fixing the transition temperature at values in the range from 350 to 450 K, demonstrating that the magnetic ordering temperature of **1** probably lies above 350 K.

[1]Department of Chemistry, University of Liverpool, Liverpool L69 7ZD, UK. [2]Materials Science Division, Department of Engineering, University of Liverpool, Liverpool L69 3BX, UK. [3]Clarendon Laboratory, Department of Physics, University of Oxford, Oxford OX1 3PU, UK. [4]ISIS Muon Facility, Rutherford Appleton Laboratory, Chilton, Didcot, Oxon OX11 0QX, UK.

*To whom correspondence should be addressed. E-mail: M.J.Rosseinsky@liverpool.ac.uk

due to chemical or crystallographic ordering, suggests they are of magnetic origin (*7*).

Magnetic long-range order in a strongly 1D structure such as the one adopted by Sr_2CuO_3 is totally unexpected at 300 K. We therefore recorded muon spin rotation (μSR) data (*8*) to investigate the behavior of the magnetic moments carried by the cobalt cations (Fig. 1A). Clear oscillations were apparent over the entire temperature range, which signified a quasi-static magnetic field at the muon site. This result demonstrates unambiguously that **1** is uniformly magnetically ordered throughout its bulk at temperatures up to at least 310 K. The amplitude of the oscillations corresponded to a signal from the whole sample, and so these results exclude the possibility that only a small region of the sample is ordered. The frequency of the oscillations approached 71 MHz as temperature (T) → 0 (corresponding to an internal field of 0.53 T) and decreased as the sample was warmed to 310 K (Fig. 1C). At the highest temperatures, the relaxation rate of the oscillations began to increase and probably reflects the approach of the phase transition (Fig. 1B). These results do not allow us to determine precisely the Néel temperature (T_N) but show that it is likely to be above 350 K. The muon site is likely to be similar to that found in Sr_2CuO_3 and Ca_2CuO_3, in which the muon is believed to form an O–μ^+ bond with a bond length of ~1 Å (*9*, *10*). However, the measured muon precession frequency for these materials is much lower, corresponding to internal fields of 2.32 and 3.5 mT for Sr_2CuO_3 and Ca_2CuO_3, respectively (*10*). Such low internal fields are associated with magnetic moments less than 0.1 μ_B (Bohr magneton). The precession frequency in the present case is >200 times greater than that in Sr_2CuO_3, which is consistent with the moment refined from powder neutron diffraction on **1**. The T_N's of Sr_2CuO_3 and Ca_2CuO_3 are ~5 and ~11 K, respectively. The much larger value of T_N observed for **1** points to a large interchain coupling, even though the lattice constants in the interchain direction are larger than those in Sr_2CuO_3 and Ca_2CuO_3.

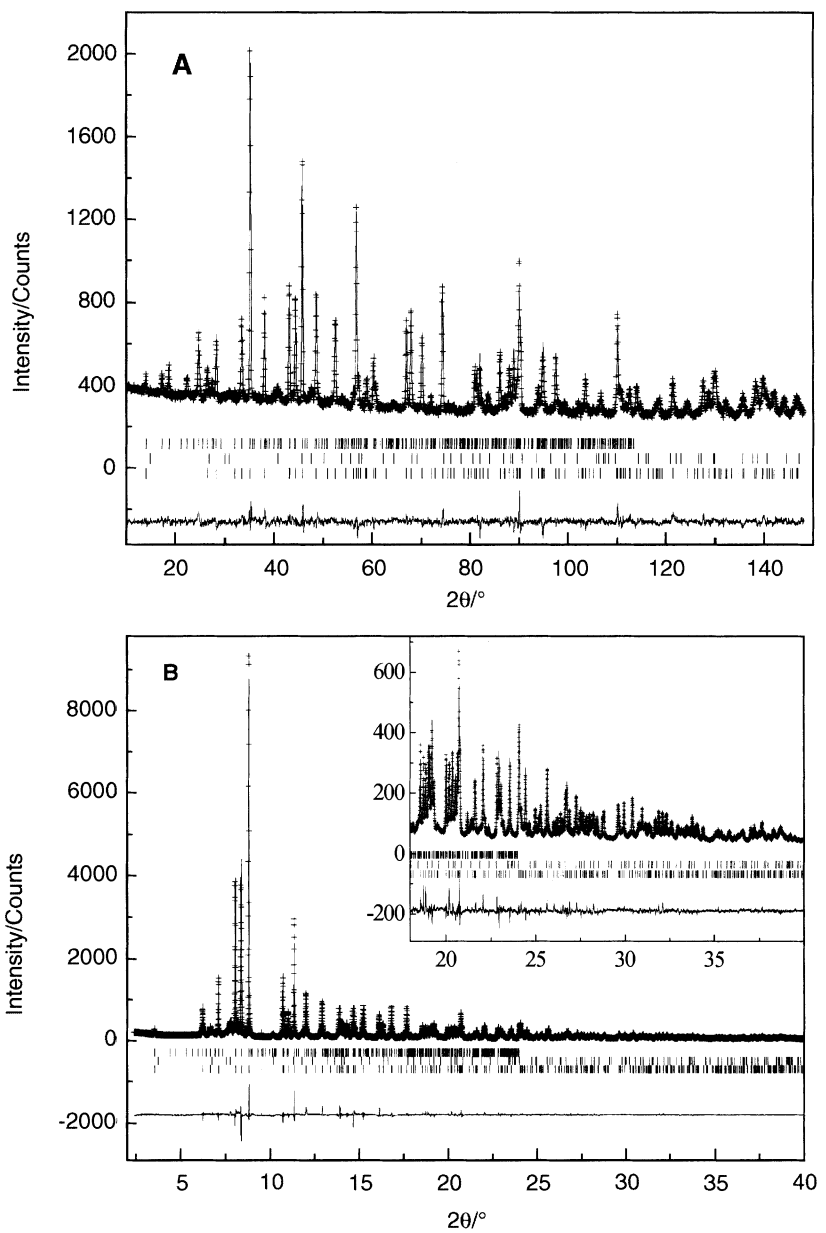

Fig. 2. Structural characterization of **1**, $LaSrCoO_3H_{0.70}$, by simultaneous Rietveld refinement of (**A**) neutron diffraction and (**B**) synchrotron XRD data collected as described in (*7*), where full refinement details are also available. **1** adopts space group *Immm*, a = 3.87093(4) Å, b = 3.60341(3) Å, c = 13.01507(10) Å, volume = 181.541(3) Å^3 La (50% occupancy)/Sr (50% occupancy) on 4*i* 0,0,0.35703(3), Co on 2*a* 0,0,0 O(1) on 4*i* 0,0,0.1673(2), O(2) on 2*b* ½, 0, 0, H on 2*d* 0,½,0 70(2)% occupancy.

After the verification of long-range magnetic order at room temperature by μSR, a simple antiferromagnetic (AF) ordering model with antiparallel spin alignment of all neighboring Co spins was incorporated into our refinement of the neutron data. Although this addition gave a satisfactory fit to the magnetic reflections, the fit to the nuclear reflections was unsatisfactory [χ^2 = 5.15, weighted-profile residual (R_{wp}) = 5.55%] (*7*). A difference Fourier map was computed and revealed a strong peak of negative scattering density at (0, ½, 0), midway between the Co atoms along the b axis at the vacant oxide anion position in the CoO_{2-x} sheets (*7*). Hydrogen is one of the few elements to have a negative neutron scattering length (*11*), and therefore hydrogen was inserted into the model at this position. The refinement immediately converged at χ^2 = 1.96 and R_{wp} = 3.43%, as shown in Fig. 2, demonstrating that **1** is the first extended transition metal oxide hydride.

The structural analysis was completed by a three-histogram refinement of 2.4 and 1.59 Å neutron histograms together with the synchrotron data (Fig. 2). The quality of the fits demonstrates the correctness of the structural model, which gives a refined composition of $LaSrCoO_3H_{0.70(2)}$. The presence of a small amount of La_2O_3 was not inconsistent with this composition (*7*). The ordered magnetic moment carried by the cobalt cations increased from 1.77(5) μ_B at 290 K to 1.95(4) μ_B at 2 K. The +1.7 oxidation state of Co deduced from the refined composition with a charge distribution assigning the –1 oxidation state to H was consistent with the position of the Co K-edge in $LaSrCoO_3H_{0.70(2)}$ (*7*), and the presence of hydride was confirmed chemically by quantitative mass spectrometric monitoring of the H_2O evolved simultaneously with oxidation of **1** under flowing O_2 at 272(5)°C, which indicates the presence of 0.4 H^- per formula unit; although necessarily less accurate than the structure refinement, this chemically confirms the presence

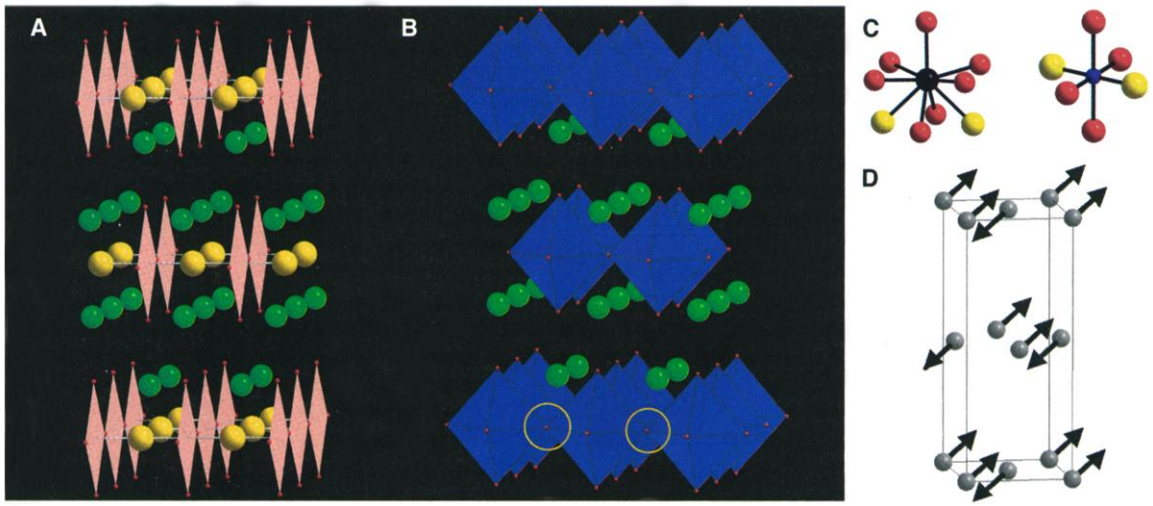

Fig. 3. (**A**) The crystal structure of **1**, $LaSrCoO_3H_{0.70}$, and its topotactic relation with (**B**) the $LaSrCoO_4$ starting material. **1** can be generated from $LaSrCoO_4$ by substitution of half of the equatorial O^{2-} anions (circled in yellow) with H^-. Hydride ions and Sr/La cations are represented as yellow spheres and green spheres, respectively; and the oxide ion arrangements around the Co cations are illustrated by squares and octahedra in (A) and (B), respectively. Co–O(1) 2.1779(22) Å × 2, Co–O(2) 1.93549(2) Å × 2, Co–H 1.80174(2) Å × 2, Sr/La–O(1) 2.469(2) Å, 2.6633(3) Å × 4, Sr/La–O(2) 2.5902(3) Å × 2, Sr/La–H 2.6849(3) Å × 2. The bond angles within the $CoO_4H_{1.4}$ unit are all constrained to 90° or 180° by the symmetry of **1**. (**C**) The coordination environments of the La/Sr (black sphere) and Co (blue sphere) sites in **1**. Oxide and hydride anions are represented as red and yellow spheres, respectively. (**D**) The magnetic structure of **1** at room temperature. For increased clarity, only the Co cations are shown. The arrows represent the direction of the ordered magnetic moments.

of hydrogen. Chemical analysis (*7*) reveals 0.26(2)% H by mass, as compared with the 0.21% expected for $LaSrCoO_3H_{0.70(2)}$.

The structure of **1** (Fig. 3) consists of chains of CoO_4 squares sharing corners along *a* to form chains that are linked into a 2D array in the *ab* plane by H^- bridges along *b*. The CoO_2 sheets in the *ab* plane of the starting material have been replaced with $CoOH_{0.7}$ sheets in the oxide hydride product, which is consistent with a reduction-insertion mechanism in which oxide vacancies are created in the *xy* plane, followed by their filling, by the H^- anions. The Co(II) cations have a mean coordination number of 5.40(4), with the H^- anions occupying the axial positions between the square plane of oxide anions. The Co–H distance of 1.80174(2) Å is shorter than either of the Co–O distances, and this, coupled with the strong covalency expected for the interaction between Co^{2+} and H^-, produces strong AF coupling between the Co(II) cations within the 2D sheets. The effect of the hydride anions on bridging the Sr_2CuO_3-like 1D chains is qualitatively demonstrated by comparing the T_N of above 300 K here with the T_N of 11 K in Sr_2CuO_3 itself. A qualitative comparison between H^- and O^{2-}oxide bridges can be made by noting that $LaSrCoO_{3.5}$ (*6*) has a Néel temperature of 110 K, with a similar concentration of bridging anions in the *ab* plane.

The high AF ordering temperature of $LaSrCoO_3H_{0.70}$ demonstrates that the H^- anion can strongly couple transition metal cations electronically. To confirm this supposition, we performed spin wave calculations to crudely model the effect of coupling the CoO_3 oxide chains through H^- anions. We find that increasing the effective exchange between chains in one direction to close to the intrachain exchange *J* is sufficient to raise T_N to the order of J/k_B (where *J* is the intrachain exchange and k_B is the Boltzman constant), even if the coupling in the orthogonal interchain direction is quite weak; the size of the moment will then be near the full value (this scenario is appropriate for $LaSrCoO_3H_{0.70}$, in which we observe a large moment, and $T_N \sim 350$ K, which is on the order of J/k_B). If, however the interchain exchange is weak in both directions, T_N is largely controlled by that weak interchain exchange, and the size of the moment is greatly reduced because of quantum fluctuations [this scenario is appropriate for Sr_2CuO_3, in which the moment is reduced to 0.06 μ_B and $T_N = 11$ K (*10*)]. This stark difference in magnetic properties highlights the crucial role played by the bridging H^- ions and confirms that they are capable of coupling transition metal centers equally as effectively as are O^{2-} anions.

The H^- anions are exclusively located in the transition metal–containing layers in the structure, in contrast to oxyhalides such as Sr_2CoO_3Cl (*3*), in which the halide anions occupy the apical positions within the electronically inactive rock salt layers. The demonstration that transition metal oxide hydrides can be isolated suggests that such species should be considered when discussing chemical and catalytic processes involving transition metal oxides, such as the spillover process (*12*) in which only H^+ and OH^- have been invoked (*13*). The site-specific insertion of the H^- anions into the oxide sheets may reflect the enhanced bridging interaction with the transition metal cations in this site, or it may be due to a topotactic transformation mechanism in which anion vacancies present in an $LaSrCoO_{3.5}$ intermediate are filled with hydride anions. The combination of cation reduction with anion insertion is unusual for a topotactic solid-state transformation but may prove to be a general route to transition metal oxide hydrides, opening up previously uncharted areas in electronic and magnetic materials synthesis. Quantitative estimates of the strength of the exchange interaction demonstrate that the H^- bridge couples metal centers as effectively as does O^{2-}, although the different frontier orbital symmetry (σ only in H^-, $\sigma + \pi$ in O^{2-}) promises that interesting property differences should be revealed in future detailed studies of this new class of extended solid.

References and Notes

1. J. B. Goodenough, J. S. Zhou, *Chem. Mater.* **10**, 14 (1998).
2. Y. D. Chuang, A. D. Gromko, D. S. Dessau, T. Kimura, Y. Tokura, *Science* **292**, 1509 (2001).
3. S. M. Loureiro, C. Felser, Q. Huang, R. J. Cava, *Chem. Mater.* **12**, 5 (2000).
4. Z. Y. Lin, M. B. Hall, *Coord. Chem. Rev.* **135**, 845 (1994).
5. M. A. Hayward, M. A. Green, M. J. Rosseinsky, J. Sloan, *J. Am. Chem. Soc.* **121**, 8843 (1999).
6. M. A. Hayward, M. J. Rosseinsky, *Chem. Mater.* **12**, 2182 (2000).
7. Full synthetic and structural characterization details are provided as supplemental data on *Science* Online at www.sciencemag.org/cgi/content/full/295/5561/1882/DC1.
8. S. J. Blundell, *Contemp. Phys.* **40**, 175 (1999).
9. A. Keren *et al.*, *Phys. Rev. B* **48**, 12926 (1993).
10. K. M. Kojima *et al.*, *Phys. Rev. Lett.* **78**, 1787 (1997).
11. G. E. Bacon, *Neutron Diffraction* (Clarendon Press, Oxford, ed. 3, 1975).
12. W. C. Conner, J. L. Falconer, *Chem. Rev.* **95**, 759 (1995).
13. S. J. Teichner, *Appl. Catal.* **62**, 1 (1990).
14. We thank the Engineering and Physical Sciences Research Council for support under GR/N21819 and for access to the Institut Laue Langevin (ILL) and the European Synchrotron Radiation Facility (ESRF); the donors of the Petroleum Research Foundation, administered by the American Chemical Society, for support; T. Hansen (ILL) and A. Fitch (ESRF) for their expert assistance with the collection of neutron and synchrotron x-ray diffraction data; the staff of the Paul Scherer Institut muon facility for their assistance with the muon experiments; L. Murphy (Synchrotron Radiation Source) for assistance with the collection of x-ray absorption data; and R. Coldea for useful discussions.

26 November 2001; accepted 24 January 2002